Steel and Composite Structures, *Vol. 36, No. 3 (2020) 307-319*
DOI: https://doi.org/10.12989/scs.2020.36.3.307

Nonlinear stability of the upper chords in half-through truss bridges

Wen Qingjie*, Yue Zixiang[a] and Liu Zhijun[b]

State Key Laboratory for Geomechanics and Deep Underground Engineering, School of Mechanics and Civil Engineering, China University of Mining & Technology, 1 Daxue Road, Xuzhou, Jiangsu province, China

(*Received May 5, 2019, Revised July 12, 2020, Accepted July 15, 2020*)

Abstract. The upper chords in half-through truss bridges are prone to buckling due to a lack of the upper transverse connections. Taking into account geometric and material nonlinearity, nonlinear finite-element analysis of a simple supported truss bridge was carried out to exhibit effects of different types of initial imperfections. A half-wave of initial imperfection was proved to be effective in the nonlinear buckling analysis. And a parameter analysis of initial imperfections was also conducted to reveal that the upper chords have the greatest impact on the buckling, followed by the bottom chords, vertical and diagonal web members. Yet initial imperfections of transverse beams have almost no effect on the buckling. Moreover, using influence surface method, the combinatorial effects of initial imperfections were compared to demonstrate that initial imperfections of the upper chords play a leading role. Furthermore, the equivalent effective length coefficients of the upper chord were derived to be 0.2~ 0.28 by different methods, which implies vertical and diagonal web members still provide effective constraints for the upper chord despite a lack of the upper transverse connections between the two upper chords. Therefore, the geometrical and material nonlinear finite-element method is effective in the buckling analysis due to its higher precision. Based on nonlinear analysis and installation deviations of members, initial imperfection of *l*/500 is recommended in the nonlinear analysis of half-through truss bridges without initial imperfection investigation.

Keywords: half-through truss bridge; aluminum alloy bridge; stability; nonlinear; influence surface

1. Introduction

Half-through truss bridges are widely used in ports, railways and rapid construction military bridges for their lower truss height, visual permeability and attractive appearance (Qingjie and Yanjun 2010, Wang 1993). However, the upper chords may easily lose stability under combined loadings due to a lack of upper transverse connections between the upper chords. The unpredictable out-of-plane buckling of upper chords may result in bridge damage before the bearing capacity of the whole bridge is reached (Birajdar *et al*. 2016, Li *et al*. 2016, Kozy *et al*. 2006). Therefore, in the structural design it is crucial to obtain calculation length of upper chord and evaluate its stability (Ye and Lu 2018).

It is well known that vertical and diagonal web members in a simply supported half-through truss bridge act as lateral restraints of the upper chords to some extent. The effective length of the upper chord cannot be achieved by use of methods in general truss structures because their desirable boundary conditions are not ideal rigid or hinge connections. The upper chord is always considered as a continuous beam with elastic lateral supports at each joint (Iwicki 2007), thus it is hard to determine the effective length theoretically. Firstly, the elastic buckling theory was used to solve the out-of-plane buckling of half-through truss bridges. Engesser (1884, 1885) solved the buckling of members with elastic lateral restraints. Lee (1958), Bleich (1952), Hu (1952), Holt (1952) and other researchers also studied the buckling of the upper chords in half-through truss bridges. To simplify analysis, the upper chord is commonly considered as a member with equivalent or parabolic axial force (Timoshenko 1961, Zhang and Huang 1998, Shang *et al*. 2008).

Based on the elastic buckling theory, several Chinese codes, TB100091 (2017), JTS152 (2012) and JTJ 283 (1999), adopt an elastic method to obtain the effective length and buckling load of an upper chord, as well as BS EN (2006), ANSI/AISC (2010) and AASHTO (2014). Meanwhile, a finite-element method (FEM) is also proposed in some specifications, whereas great difference in the FEM analysis was identified between the elastic and nonlinear results. Elastic results were significantly different from the experimental values (Liu *et al*. 2007). However, taking into account geometric and material nonlinearity, the calculated buckling loads and modes were both in good agreement with the experimental values (Jankowska-Sandberg *et al*. 2013). Hence the nonlinear EFM is recommended in ANSI/AISC (2010), AASHTO (2014) and JTG D64 (2015), yet the detailed procedure is not presented. In effect, both the amplitude and the form of initial defects have essential effects on structural stability (Smyrnaios *et al*. 2015, Iwicki 2007, Habibi and Bidmeshki 2018). And the first order buckling mode is always introduced into

*Corresponding author, Associate Professor
E-mail: cumtwenqingjie@126.com
[a]Ph.D. Student
E-mail: viscarialight@126.com
[b]Associate Professor
E-mail: liuzhijun0331@163.com

ISSN: 1229-9367 (Print), 1598-6233 (Online)

Fig. 1 A half-through aluminum alloy truss bridge located in Hangzhou

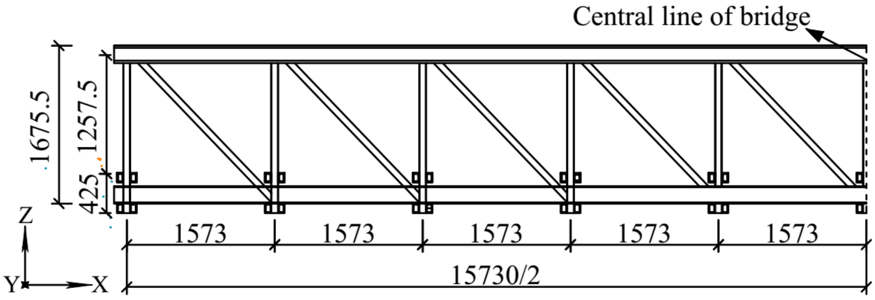

Fig. 2 Elevation of a half span of a truss bridge (unit/mm)

nonlinear stability analysis as initial imperfections. Due to significant impact of initial imperfections, to identify appropriate initial imperfections is very useful in calculating the limit buckling load of the upper chord.

The purpose of the study is to discuss effects of initial imperfections in finite-element analysis by comparing of geometric nonlinearity with different initial imperfections. Meanwhile, parameter and influence surface analysis of a half-through truss bridge were carried out to determine sensitivity of different types of initial imperfections. Based on nonlinear finite-element results and field investigation on initial imperfections, both the amplitude and the form of initial imperfections were discussed to identify appropriate initial imperfections in the nonlinear analysis of half-through truss bridges. Furthermore, the constraint effects of vertical and diagonal web members were evaluated by the effective or equivalent length coefficient of the upper chord derived from Euler equation.

2. Numerical example

To carry out the research, a half-through aluminum alloy truss bridge located in Hangzhou, China, as illustrated in Fig. 1, was used as a numerical example. As shown in Figs. 2 and 3, this simple supported truss bridge has a span of 15.73 m, a full width of 3.48 m, and a total height of 1.675 m. The upper and lower chords are divided into 10 equal parts in length by web members, and the internodal length is 1.573 m. The length of each diagonal web member is 2.264 m, and the transverse frame is 0.425 m in height. The height from the centroid of a top chord to the top surface of a transverse frame is 1.258 m, and the height from the top surface of a transverse beam to the centroid of a transverse frame is 0.213 m. Double U-shape section is adopted in the upper and lower chords, and thin-walled box sections are used in all other members. Table 1 illustrates section parameters of all the members based on coordinate axis in Fig. 2.

Aluminum alloy 6082 T6 with Young's modulus E of 71 GPa, poisson ratio v of 0.3, and density ρ of 2700 kg/m^3, is used in all the members of the truss bridge. Aluminum alloy has no obvious yield point, hence the stress of 0.2% plastic residual strain is generally considered as yield strength. The yield strength $f_{0.2}$ is 260 MPa, and the ultimate strength f is 310 MPa. Based on the cross-sectional areas listed in Table 1, the yield and ultimate axial forces in the upper chord were calculated to be 1454.96 kN and 1734.76 kN, respectively. The live load of pedestrians on the bridge deck is set to 4.625 kN/m^2 according to the Chinese footbridge design code.

3. Eigenvalue buckling analysis

Initial imperfections in nonlinear buckling analysis are mostly taken from eigenvalue buckling deformations when structural defects cannot be detected (Mazzolani 1995, Habibi and Bidmeshki 2018). Based on the supposition of small deformation and elastic material, eigenvalue buckling analysis is firstly used to obtain initial structural defects so

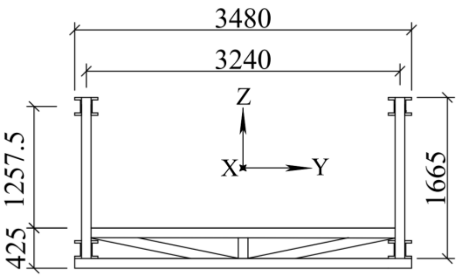

Fig. 3 Transverse section of a truss bridge (unit/mm)

Table 1 Section parameter of members

component	Section width (m)	Section height (m)	Section area (m^2)	Section moment of inertia I_x (m^4)	Section moment of inertia I_y (m^4)	Section moment of inertia I_z (m^4)
Upper/bottom chords	0.244	0.185	5.596×10^{-3}	/	2.594×10^{-5}	2.895×10^{-5}
Web members	0.1	0.07	2.464×10^{-3}	/	3.166×10^{-6}	3.380×10^{-6}
Upper transverse members of the transverse frame beam	0.21	0.1	4.916×10^{-3}	5.78×10^{-5}	/	6.332×10^{-6}
Bottom transverse members of the transverse frame beam	0.21	0.1	4.916×10^{-3}	5.78×10^{-5}	/	6.332×10^{-6}
Web members of the transverse frame beam	0.07	0.1	2.464×10^{-3}	3.166×10^{-6}	/	3.380×10^{-6}

Table 2 Critical buckling loads and buckling half-wave number

Modal order	Critical buckling load/kN	Half-wave number	Modal order	Critical buckling load/kN	Half-wave number
1	1696.4	2	7	2891.3	4
2	1704.7	3	8	3275.7	5
3	1880.2	3	9	3690.8	5
4	1944.3	4	10	4473.5	6
5	2635.1	4	11	4676.8	6
6	2743.7	5	12	4821.7	7

as to conduct nonlinear analysis. Using the FEM, the first-order to twelfth-order buckling modes were obtained and listed in Fig. 4. Critical buckling loads and buckling half-wave number of the upper chord were also shown in Table 2.

Fig. 4 and Table 2 show that both buckling half-wave number and critical buckling load increase with the growth of the modal order. Besides buckling deformation of the upper chords, lateral bending and twisting of the whole truss bridge were also detected in the first-, second-, fifth-, sixth-, ninth-, and tenth-order buckling mode. Except the buckling modes above, the other six modes of the twelve modes were listed to exhibit symmetrical buckling deformation of the upper chord. Critical buckling load of the third-order mode is 1880.2 kN, almost equal to the elastic theoretical result of 1843 kN without lateral bending and twisting deformation. And the third-order buckling mode also agrees with theoretical results without considering the overall deformation of the truss bridge. Critical buckling load of the first-order mode is 9.8% smaller than the theoretical result, which has higher precision because the overall deformation of the truss is considered. Therefore, the FEM is also recommended to obtain critical buckling load in some design specifications, besides the elastic theoretical methods.

4. Nonlinear buckling analysis

To investigate practical mechanical state of a half-through truss bridge, further nonlinear buckling analysis is needed to analyze the influence of geometrical and material nonlinearity. Based on R-O model presented by Osgood W. R. in 1943 (Mazzolani 1995), stress-strain relation curve of aluminum alloy 6082 T6 is derived as shown in Fig. 5 to

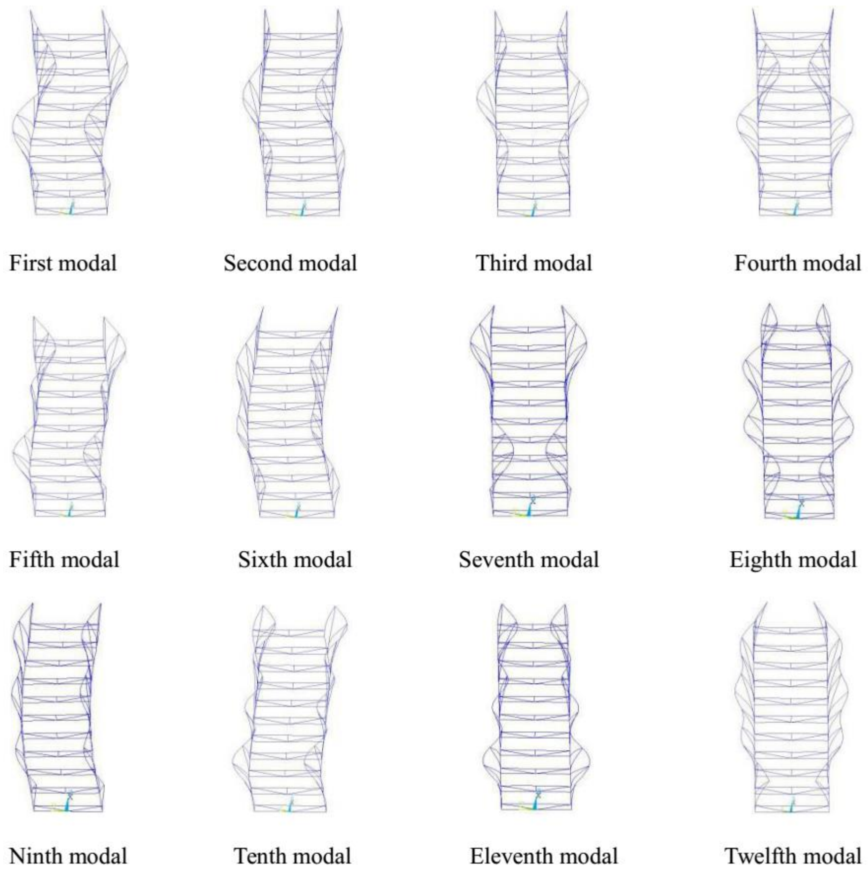

Fig. 4 Eigenvalue buckling modes

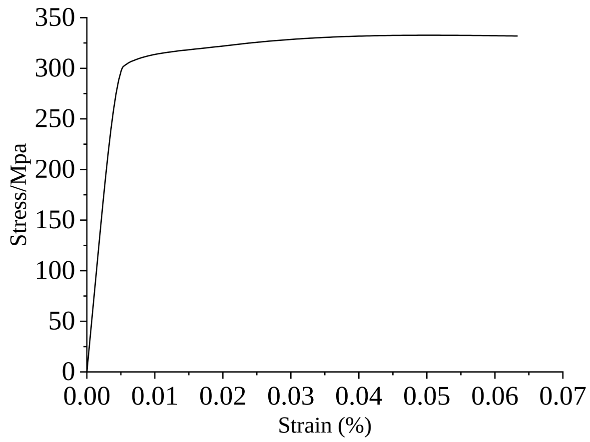

Fig. 5 Stress-strain relation curve of aluminum alloy 6082 T6

conduct nonlinear buckling analysis by use of ANSYS software.

4.1 Initial imperfection form

The first eigenvalue buckling mode can be introduced into structural nonlinear analysis as initial imperfection (Tomás *et al*. 2012, Habibi and Bidmeshki 2018). Nevertheless, the most disadvantaged geometric deficiencies are not always in accordance with the first modal shape according to previous literatures (Jiang *et al*. 2011). So it is necessary to compare buckling performance of the truss bridge with different initial imperfections derived from the eigenvalue buckling modes (Szymczak

Table 3 Calculated limit loads with different initial imperfection

Number	Types of imperfection	Limit load with geometrical and material nonlinearity /kN	Limit load with geometrical nonlinearity /kN
1	None imperfection	1737	1905
2	One-half-wave imperfection	1241	1346
3	Mode 1(two-half-wave imperfection)	1276	1415
4	Mode 2(three-half-wave imperfection)	1255	1406
5	Mode 3(three-half-wave imperfection)	1302	1573
6	Mode 4(four-half-wave imperfection)	1365	1643
7	Mode 5(four-half-wave imperfection)	1412	1662
8	Mode 6(five-half-wave imperfection)	1391	1557
9	Mode 7(four-half-wave imperfection)	1421	1731
10	Mode 8(five-half-wave imperfection)	1421	1595
11	Mode 9(five-half-wave imperfection)	1420	1489
12	Mode 10(six-half-wave imperfection)	1448	1715
13	Mode 11(six-half-wave imperfection)	1445	1663
14	Mode 12(seven-half-wave imperfection)	1452	1593

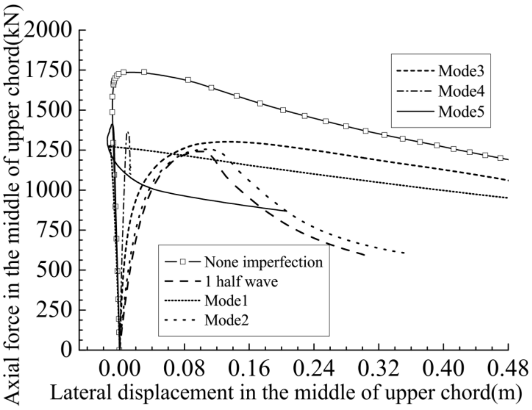

(a) Load-displacement curves with number 1 - 7

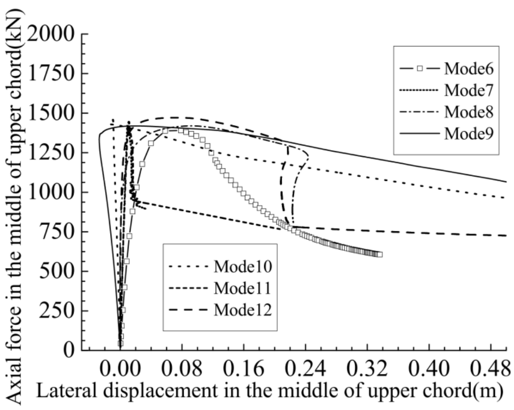

(b) Load-displacement curves with number 8 - 14

Fig. 6 Load-displacement curves of the upper chord

and Kujawa 2017, Mehdi and Hossein 2017).

Although Table 2 shows that two half-waves is the minimum number of all the eigenvalue buckling modes with multi internodes, one-half-wave buckling mode still probably appears in the half-through truss bridges. Thus, one-half-wave modal shape of the upper chord can also be considered as the initial imperfection in nonlinear buckling analysis. Likewise, one thousandth of the span l is considered as the largest initial imperfection of the buckling modal shape. Besides, nonlinear buckling analysis of the whole truss bridge can also be conducted without initial imperfections. Geometrical and material nonlinearity were analyzed by use of ANSYS software to investigate their effects, respectively. The calculated limit loads are listed in Table 3, and load-displacement curves with geometrical and material nonlinearity are demonstrated in Fig. 6. Meanwhile, buckling modal shapes with and without initial imperfections are both illustrated in Fig. 7 to exhibit pre-buckling and post-buckling waveforms.

Table 3 shows that limit load of the upper chord will reach 1905 kN when only geometrical nonlinearity is taken into account without initial imperfections. It is very close to the eigenvalue buckling load of the third-order mode, which indicates that geometrical nonlinear result without initial

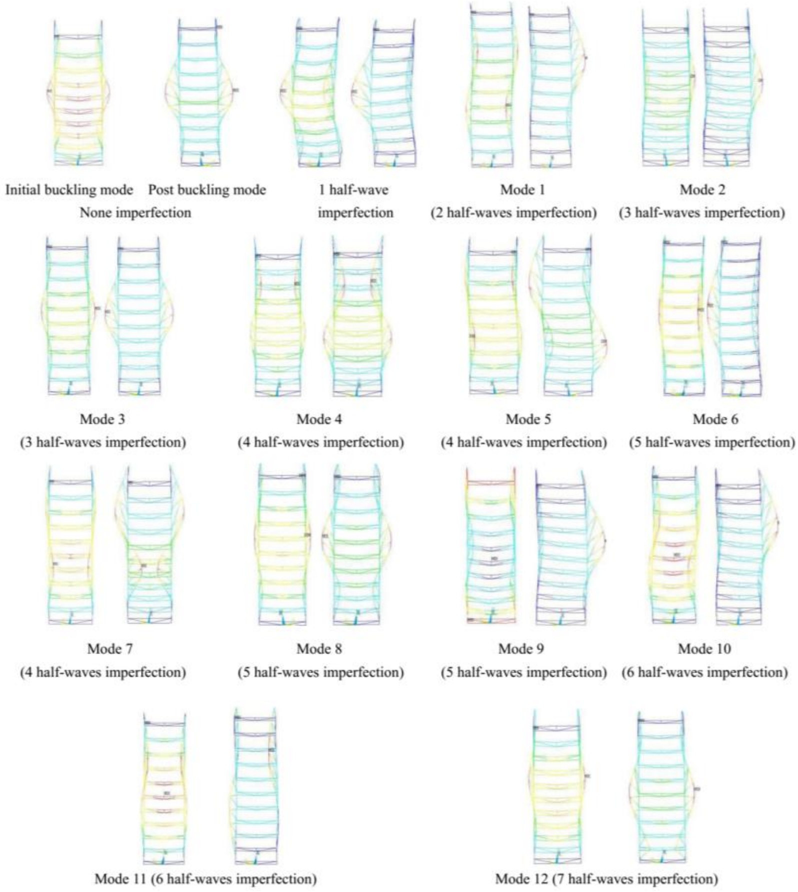

Fig. 7 Pre-buckling and post-buckling waveforms of the truss bridge

imperfections is similar to the elastic buckling analysis. Meanwhile, the limit load of geometrical nonlinearity with 1/1000 initial imperfections decreases largely due to initial imperfections, and especially for one-half-wave imperfection the limit load reduces by 30%. In addition, the limit load rises with increasing half-wave number. In view of geometrical nonlinearity, elastic results cannot reveal the real structural buckling stability since initial imperfections are always inevitable.

Material nonlinearity also has a similar marked influence on the limit load. When both geometrical and material nonlinearity are taken into account, the limit loads are 8%~18% lower than the calculated results with only geometrical nonlinearity. In other words, material nonlinearity undertakes a 8%~18% decrease in the limit load. As illustrated in Table 3, limit loads of the truss bridge with initial imperfections are significantly lower than that without initial imperfections. In effect, geometrical and material nonlinear analysis of the half-through truss bridge is necessary in buckling analysis.

Fig. 6 demonstrates that the displacement of the model with initial imperfection of even-numbered half-wave climbs approximately in a line with increasing axial force in the upper chord, and then drops abruptly after the peak, appearing as a secondary bifurcation buckling. However, the load-displacement curves of the models without initial imperfections but with odd-numbered half-wave exhibit a slowly rising trend before the peak and a slow decline after the peak, namely extreme point buckling.

As shown in Fig. 7, when initial imperfections of different half-waves are considered in the FEM, pre-buckling waveforms of the upper chords always exhibit two or three half-waves. Especially when initial imperfections of twisting are input, post-buckling waveforms indicate a trend of development to one half-wave. In other words, pre-buckling and post-buckling waveforms with different initial imperfections imply a spontaneous development to a lower order during the pre and post buckling. Based on energy method used in theoretical buckling analysis of the upper chord (Wen *et al*. 2018), higher-order buckling deformation implies greater deformation energy, thus greater work done by axial force is needed during the buckling of the upper chord. To improve the efficiency of the work due to axial force, buckling deformation with higher-order initial imperfection will approach the lowest order initial imperfection. Therefore in nonlinear buckling analysis it may be more effective to adopt the lowest-order mode, one half-wave, as initial imperfection due to its efficiency in modeling.

In addition, the pre and post buckling deformations in reverse direction of the upper chords are identified in some modes with initial imperfections. As shown in Fig. 8,

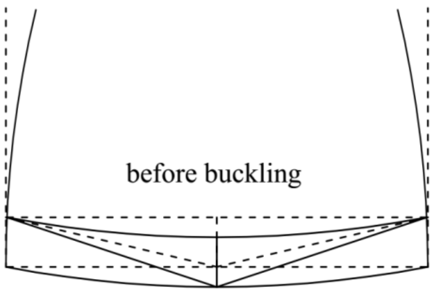

(a) Pre buckling deformation

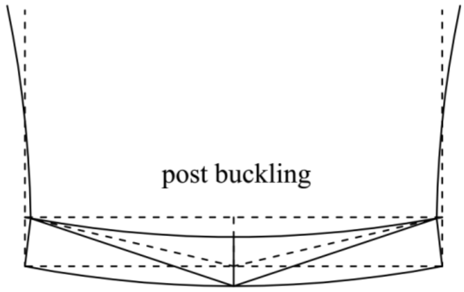

(b) Load-displacement curves with number 8 - 14

Fig. 8 Deformation of the transverse section pre and post buckling

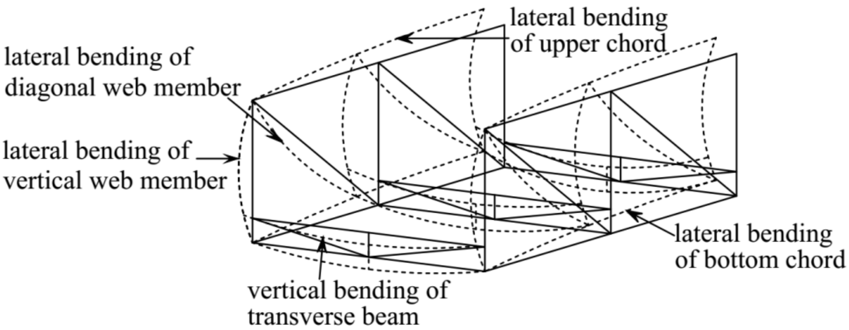

Fig. 9 Initial imperfections of the half-through truss bridge

vertical web members and the frames formed by vertical web members and transverse beams deflect towards inside before buckling, yet they may deflect towards outside after buckling. It is mainly caused by the twisting and bending deformations of the vertical web members of the truss.

4.2 Parameter analysis of initial imperfections

Besides lateral bending deformation of the upper chords, half-through truss bridges may have many other types of initial imperfections. Based on practical measurements, six main types of initial imperfections in Fig. 9 are listed as below: (1) lateral bending of the upper chords; (2) lateral bending of the bottom chords; (3) lateral bending of the vertical web members at bridge bearings; (4) lateral bending of all vertical web members; (5) lateral bending of all diagonal web members; (6) vertical bending of all transverse beams. Parameter analysis of different type of initial imperfection is in need to investigate the effect of initial imperfection.

In geometric and material nonlinear analysis, one-half-wave mode was chosen as initial imperfection, and the initial deformations of the six types of initial imperfection were taken as 0, l/1000, l/500, l/300, l/200 and l/100 of the buckling modal deformation separately, where l is the span of the truss bridge. The six types of initial imperfections were introduced into the whole truss bridge to conduct geometric and material nonlinear buckling analysis by use of ANSYS software, and load-displacement curves were obtained as shown in Fig. 10.

Fig. 10 demonstrates that load-displacement curve without initial imperfections develops almost linearly before peak point with increasing lateral displacement towards the inner side of the upper chords as shown in Fig. 8. The lateral displacement of the upper chord reaches 0.03 m at the peak. And then it turns to the opposite direction. When the lateral displacement remains rising towards the outside, axial forces in the upper chords follow a nearly steady decline. Compared with the theoretical buckling load, the buckling loads drop down at different levels when initial imperfections are considered in nonlinear analysis.

Considering the initial imperfection of lateral bending of the upper chords, the nonlinearity of the load-displacement curve grows with increasing initial imperfection. And the curve becomes more and more flat in the rising and falling phrase as shown in Fig. 10 (a). When initial imperfection of l/100 is considered on the upper chords, the maximum lateral displacement of the upper chord reaches 0.125m at the peak, and the buckling load reduces by 58.2% compared with finite-element mode without initial imperfection, which is far less than elastic theoretical value of 1843kN.

Considering initial imperfection of lateral bending of the bottom chords, the load-displacement curves in Fig. 10 (b) are similar to that in Fig. 10 (a), while the lateral buckling deformation of the upper chords is greater during buckling. The maximum lateral displacement of the upper chord reaches 0.175m at the peak when initial imperfection of l/100 is considered on the bottom chords. And the buckling load reduces by 41.2%, compared with the finite-element mode without initial imperfection. Initial imperfection of

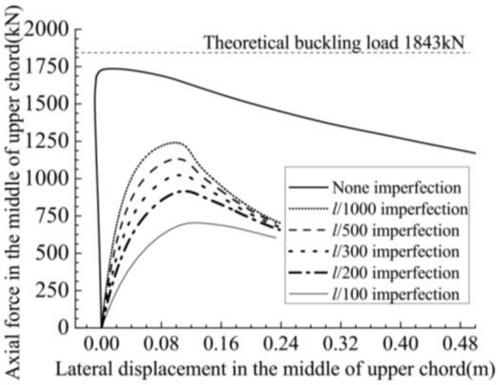

(a) Initial imperfection of lateral bending of upper chords

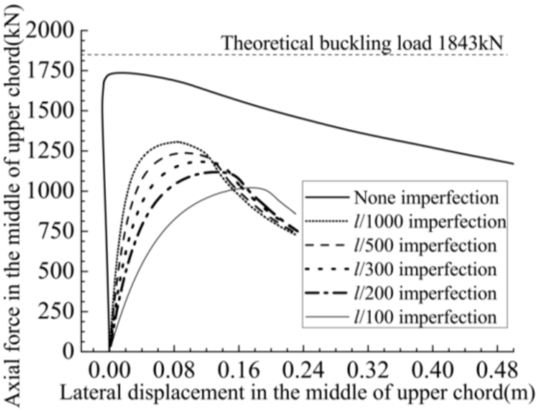

(b) Initial imperfection of lateral bending of bottom chords

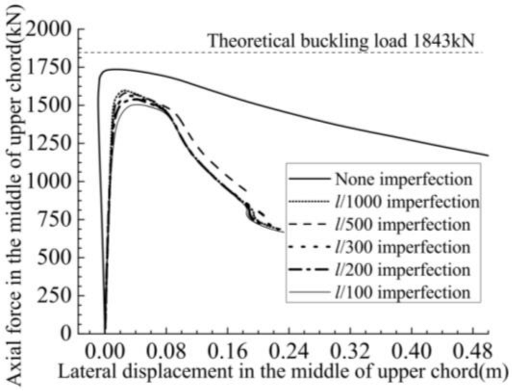

(c) Initial imperfection of lateral bending of four vertical web members at supports

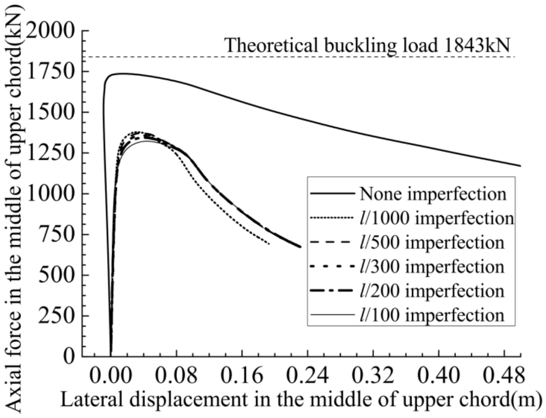

(d) Initial imperfection of lateral bending of all vertical web members

Continued-

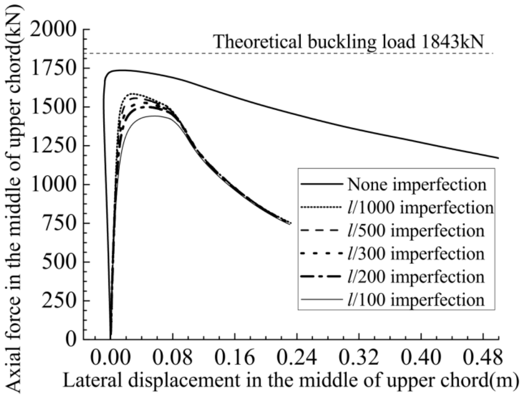

(e) Initial imperfection of lateral bending of all diagonal web members

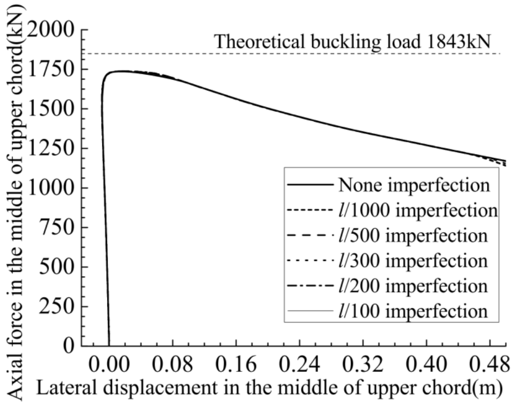

(f) Initial imperfection of vertical bending of all transverse beams

Fig. 10 Load-displacement curves of the upper chord

the bottom chords has a slightly less influence on buckling than that of the upper chords.

When initial imperfections of the lateral bending of the vertical web members at bridge bearings are considered, the load-displacement curve in climbing phase is similar to that without initial imperfection, but the lateral displacement remains on increasing outwards as shown in Fig. 10(c). Meanwhile, the buckling load declines sharply after the peak. Compared with the FEM without initial imperfection, the buckling load reduces by 13.3% when initial imperfection of *l*/100 is introduced into analysis. Therefore, the four vertical web members at bridge bearings are very sensitive to buckling of the upper chords.

When initial imperfection of the lateral bending of all vertical web members is considered, the load-displacement curve in Fig. 10(d) is very close to that in Fig. 10(c). Nevertheless, the buckling load reduces by 23.4% when initial imperfection of *l*/100 is introduced, which is about 10 percent lower than that in Fig. 10(c). It means vertical web members except the four ones at bridge bearings only contribute 10% to the reducing of the buckling load. In any case, much attention should be paid when initial imperfections in many vertical web members are determined.

Similarly, the load-displacement curve in Fig. 10(e) exhibits a better climbing linearity when initial imperfection of the lateral bending of all diagonal web members is taken into account. However, buckling loads fluctuate greatly near the peak and the curves with different levels of initial imperfection's overlap in the descending phase. The buckling load reduces by 16.9% at most when initial imperfection of *l*/100 is considered.

Fig. 9(f) demonstrates that all the load-displacement curves overlap in spite of initial imperfections. It means that vertical bending of all transverse beams has almost no effect on buckling feature.

In summary, of all initial imperfections the upper chord is the most significant and its amplitude has the greatest impact on the buckling performance of the upper chord. The buckling load of the upper chord with imperfection of *l*/500 is 1134kN, yet it even decline 58.2% when the imperfection of *l*/100 is considered. Besides, the bottom chords also have a great effect on the buckling load. Although the effects of vertical and diagonal web members are limited, they still cannot be ignored in nonlinear analysis of half-through truss bridges. Nevertheless, initial imperfection of all transverse beams is the most likely to be neglected.

4.3 Combinatorial analysis of initial imperfections

In half-through truss bridges more than one initial imperfection may take effect simultaneously, thus combinatorial analysis is necessary to ensure that unfavorable combination of the buckling is considered. Based on the above parameter analysis, the most disadvantageous initial imperfection is lateral bending of

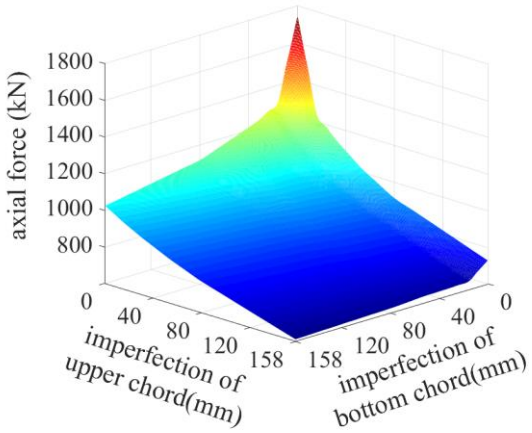

(a) Lateral bending of both upper and bottom chords

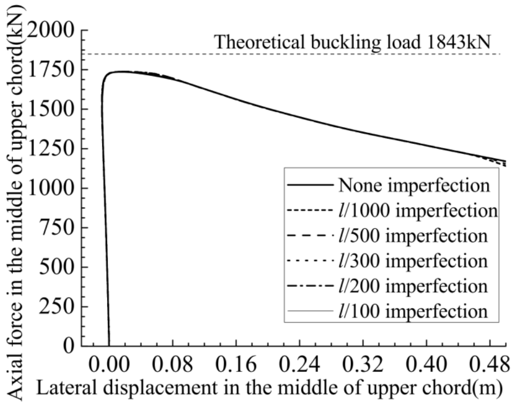

(b) Lateral bending of both upper chords and all vertical web members

Fig. 11 Influence surface with combined two initial imperfections

the upper chords, followed by lateral bending of the bottom chords, lateral bending of vertical web members, and lateral bending of all diagonal web members. Since lateral bending of all diagonal web members has the least impact besides vertical bending of transverse beams, it is negligible in combinations. Accordingly, lateral bending of the upper chords was combined with lateral bending of the bottom chords and lateral bending of vertical web members, separately. And then geometrical and material nonlinear analysis was carried out with combined initial imperfections of 0, *l*/1000, *l*/500, *l*/300, *l*/200 and *l*/100 to obtain curves surfaces in Fig. 11 by use of MATLAB software.

Fig. 11 shows that the amplitude of initial imperfection has a great influence on the buckling loads. In Fig. 11 (a) the buckling load of the upper chords without initial imperfection reaches 1737 kN at the peak. However, the buckling load drops dramatically once combined initial imperfections are considered. The reduction of the buckling load decrease gradually with increasing combined initial imperfections. When the two initial imperfections are both taken as *l*/100, buckling load the upper chord is 612.86 kN, which is only about 35.2% of the value without initial imperfection and is 6.6% lower than that of the finite-element model with initial imperfection of the upper chords. It is obvious that initial imperfection of the upper chords play a dominant role in the reduction of buckling loads. Especially when initial imperfection reaches about 31.5 mm, or *l*/500, initial imperfection of the bottom chords has little effect on buckling loads.

Buckling load of the combined initial imperfections of the upper chords and vertical web members exhibits a similar trend as shown in Fig. 11(b), while initial imperfection of vertical web members has much less impact on the buckling load. Only when initial imperfection of the upper chord is below 20mm, or *l*/787, will vertical web members demonstrate a relatively obvious effect. When the two initial imperfections are both taken as *l*/100, buckling load of the upper chord is 636.8 kN, which is only about 36.6% of the value without initial imperfection and is only 5.2% lower than that of the finite-element model with initial imperfection of the upper chords. Analysis of the influence surface indicates that the buckling load drops slowly with increasing initial imperfections when initial imperfection exceeds *l*/500.

In fact, there are different allowable deviations in different codes. In BS EN (2006), from *L*/100 to *L*/300 of initial local imperfection is recommended in the plastic analysis, where *L* is the member length. However, allowable bending deviation of beam *L*/1000 is required in Chinese code for construction quality acceptance of aluminum alloy structures. Compression, tension and web members of the truss can have allowable initial imperfection of *L*/1000, *L*/500 and *L*/300 separately in the Chinese technical standard of maintenance for city bridges.

Table 4 Effective (equivalent) length and coefficient of different methods

Calculate methods	Critical (limit) buckling load P_{cr} (kN)	Effective (equivalent) length l_c (m)	Effective (equivalent) length coefficient μ
Theoretical method	1843	3.318	0.211
Elastic FEM	1696	3.458	0.220
geometrical and material nonlinearity without initial imperfections	1713	3.441	0.219
geometrical and material nonlinearity with initial imperfection of one half-wave(l/1000)	1224	4.071	0.259
geometrical and material nonlinearity with initial imperfection of one half-wave(l/500)	1118	4.260	0.271

Compression members and lateral bending height of the truss can have allowable bending deviation of L/1000 in the Chinese code for construction quality acceptance of steel structures. As far as the upper chord is concerned, the span of L is equal to the member length of l. In addition, based on field investigation of aluminum alloy truss bridges, most initial imperfections of the members due to installation deviation are less than l/500, which is within the scope of the codes. In nonlinear analysis, installation deviation is more important than initial imperfections based on eigenvalue buckling modes (Mehdi and Hossein 2017). Combined with nonlinear analysis of initial imperfections subject to eigenvalue buckling and allowable installation deviation of members, initial imperfection of l/500 may be taken as a suggested value in nonlinear analysis to obtain buckling loads.

5. Effective length coefficient

The effective length coefficient of the upper chord depends on its effect of the constraints, which have an important effect on the elastic stability of the upper chord. It can be obtained from Eq. (1) below.

$$\mu = \frac{\pi}{l}\sqrt{\frac{EI}{P_{cr}}} \tag{1}$$

Where the length of the upper chord $l=l_c/\mu$, l_c is the effective length, and μ is the effective length coefficient.

To compare with elastic results and avoid unsafe aluminum alloy bridge design based on elastic theory, equivalent length coefficients of the upper chord can be achieved using Eq. (1) similarly. The equivalent length coefficient based on nonlinear analysis is useful as a reference in the structural design of similar half-through truss bridges. Limit loading of the upper chord is estimated and the section parameters are preliminary determined without complex computation. Therefore, taking the half-through aluminum alloy truss bridge in Fig. 1 as an example, the computed elastic and nonlinear results are all listed in Table 4.

Table 4 shows that limit buckling loads, equivalent lengths and coefficients of the upper chord using the nonlinear FEM with initial imperfection drop greatly compared with other methods. The calculated effective or equivalent lengths are from 3.316 m to 4.227 m, which are almost equal to two or three internodal lengths. And effective or equivalent length coefficients vary from 0.210 to 0.269, which are far less than 1.0. The effective or equivalent length coefficient of the upper chord reflects the constraint effect of web members, which is important in the section design of the upper chord. The calculated results imply that vertical and diagonal web members provide effective constraints for the upper chord despite a lack of the upper cross connections between the two upper chords. Nevertheless, the constraint effect of the vertical and diagonal web members is only about from 21% to 27% of hinge joints. To improve the constraint effect, it is an effective way to reduce effective or equivalent length coefficient μ by increasing the number of web members or enlarging the section area.

Of all the methods, nonlinear result without initial imperfections is very close to the elastic finite-element results. Yet initial imperfection of l/1000 and l/500 increase the effective or equivalent length coefficient of the upper chord by 118% and 123%, respectively. In design, larger μ is safer for the half-through truss bridge. Since there is no much difference in the effective or equivalent length coefficients between l/1000 and l/500, l/500 imperfection of the upper chord is more practical in the nonlinear analysis for the safety of half-through aluminum alloy truss bridges.

6. Conclusions

A numerical simulation of a simple supported half-through truss bridge was carried out to discuss its nonlinear stability. And some meaningful conclusions were given as follows.

- Based on eigenvalue buckling modes, l/1000 initial imperfection is taken into account in nonlinear buckling analysis to achieve buckling loads, load-displacement curves and buckling modes. Lateral bending deformation of lower order mode is proved to be the most effective initial imperfection in geometrical nonlinear analysis. And one half-wave is suggested as initial imperfection in nonlinear buckling analysis.
- Material nonlinearity has a marked influence on limit buckling load and undertakes a decrease of 8%~18% in the buckling loads. Parameter analysis of initial

imperfections indicates that the upper chords have the greatest impact on buckling load, followed by the bottom chords, vertical and diagonal web members. Initial imperfection of transverse beams almost has no effect on buckling features. Analysis of influence surface indicates the upper chords play a leading role in combinatorial analysis of initial imperfections.

- Numerical results of a general half-through truss bridge demonstrate the effective or equivalent length of the upper chord is almost equal to two or three internodal lengths, and the effective or equivalent length coefficient is about 0.2~ 0.28. Despite a lack of the upper cross connections between the two upper chords, vertical and diagonal web members still provide effective constraints for the upper chord. To improve the constraint effect, it is an effective way to reduce effective or equivalent length coefficient μ by increasing web members or enlarging the cross-sectional area.
- Geometrical and material nonlinear FEM is recommended to obtain the buckling load of a half-through truss bridge due to its high precision. In the absence of initial imperfection investigation, initial imperfection of l/500 is suggested based on nonlinear analysis of initial imperfection subject to eigenvalue buckling and allowable installation deviation of members.

Acknowledgments

The authors wish to express their gratitude and sincere appreciation to Fundamental Research Funds for the Central Universities (2017XKQY050) for financing this research work.

References

AASHTO (2014), *AASHTO LRFD Bridge Design Specifications* (7th Ed.), American Association of State Highway and Transportation Officials; Washington DC, USA.

ANSI/AISC 306-10 (2010), Specification for Structural Steel Buildings, American Institute of Steel Construction; Chicago, USA.

Birajdar, H.S., Maiti P.R. and Singh, P.K. (2016), "Strengthening of Garudchatti bridge after failure of Chauras bridge", *Eng. Fail. Anal.*, **62**, 49-57. https://doi.org/10.1016/j.engfailanal.2015.12.002.

Bleich, F. (1952), *Buckling Strength of Metal Structures*, McGraw-Hill Book Company, New York, USA.

BS EN 1993-2 (2006), Design of Steel Structures. Part 2: Steel bridges, European Committee for Standardization; Brussels, Belgium.

Engesser, F. (1884, 1885), *Die Sicherung offener Brucken gegen Ausknicken*. Zentralbatt der Bauverwaltung, Deutschland. [In German]

Habibi, A. and Bidmeshki, S. (2018), "A dual approach to perform geometrically nonlinear analysis of plane truss structures", *Steel Compos. Struct.*, **27**(1), 13-25. https://doi.org/10.12989/ scs.2018.27.1.013.

Holt, E.C. (1952), "Buckling of a Pony Truss Bridge", in Stability of Bridge Chords without Lateral Bracing, Rep. No. 2; Column Research Council, Bethlehem, PA, USA.

Hu, L.S. (1952), "The Instability of Top Chords of Pony Trusses", Dissertation, University of Michigan, Ann Arbor, Michigan.

Iwicki, P. (2007), "Stability of trusses with linear elastic side-supports", *Thin-Wall. Struct.*, **45**(10), 849-854. https://doi.org/10.1016/j.tws.2007.08.005.

Jankowska-Sandberg, J. and Kołodziej, J. (2013), "Experimental study of steel truss lateral–torsional buckling", *Eng. Struct.*, **46**(46), 165-172. https://doi.org/10.1016/j.engstruct.2012.07.033.

Jiang Z.R., Shi K.R. and Xu, M. (2011), "Analysis of nonlinear buckling and construction simulation for an elliptic paraboloid radial beam stringstructure", *China Civil Eng. J.*, **44**(12), 1- 8. https://doi.org/10.15951/j.tmgcxb.2011.12.009.

JTG D64-2015 (2015), Specification for Design of High way Steel Bridge, Ministry of Transport of People's Republic of China; Beijing, China.

JTJ 283-1999 (1999), Code for Design of Steel Structure in Port Engineering, Ministry of Transport of People's Republic of China; Beijing, China.

JTS152-2012 (2012), Code for Design of Steel Structures in Port and Waterway Engineering, Ministry of Transport of People's Republic of China; Beijing, China.

Kozy, B., Boyle, R. and Earls, C.J. (2006), "Chord bearing capacity in long-span tubular trusses", *Steel Compos. Struct.*, **6**(2),103-122. https://doi.org/10.12989/scs.2006.6.2.103.

Lee, S.L. and Clough, R.W (1958), "Stability of pony truss bridges", *Bridge Struct. Eng.*, **18**, 91

Li, R. Yuan, X., Yuan, W., Dang, X. and Shen, G. (2016), "Seismic analysis of half-through steel truss arch bridge considering superstructure", *Struct. Eng. Mech.*, **59**(3), 387-401. https://doi.org/10.12989/sem.2016.59.3.387.

Liu liangmou and Xu Guanyao (2007), "Testing study on the global stability of "321" prefabricated highway steel bridge", *Steel Construction*, 4, 59-61.

Mazzolani, F.M. (1995), *Aluminum Alloy Structure* (2nd Ed.), Taylor & Francis Group, Chapman & Hall, London, England.

Rastgar, M. and Showkati, H. (2017), "Buckling of cylindrical steel tanks with oblique body imperfection under uniform external pressure", *J. Pressure Vessel Technol.*, **139**(6), 1-11. https://doi.org/10.1115/1.4037808.

Shang Xiaojiang, Xiao Congzhen, and Zhang Liruo (2008), "Discuss on out-plane effective length of compressive chord members in truss without lateral supports", *Build. Struct*., **38**(6), 93-98. https://doi.org/10.3901/JME.2008.05.160.

Smyrnaios, S.V., Iliopoulos, A. and Vayas, I. (2015), "Truss models for inelastic stability analysis and design of steel plate girders", *Eng. Struct*., **105**, 65-173. https://doi.org/10.1016/j.engstruct. 2015.09.040.

Szymczak, C. and Kujawa, M. (2017), "Buckling of thin-walled columns accounting for initial geometrical imperfections", *Int. J. Nonlinear Mech.*, **95**, 1-9. https://doi.org/ 10.1016/j.ijnonlinmec.2017.06.003.

TB100091 (2017), Code for Design of Steel Structure of Railway Bridge, Ministry of Transport of People's Republic of China; Beijing, China.

Timoshenko Gere (1961), *Theory of elastic stability* (2nd Ed.), McGraw- Hill Book Company, New York, USA.

Tomás, A. and Tovar, J.P. (2012), "The influence of initial geometric imperfections on the buckling load of single and double curvature concrete shells", *Comput. Struct*., **96-97**, 34-45. https://doi.org/10.1016/j.compstruc.2012.01.007.

Wang, T.L. (1993), "Impact in railway truss bridge", *Comput. Struct*., **49**(6), 1045-1054. https://doi.org/10.1016/0045-7949(93)90016-7.

Wen, Q.J. and Qi, Y.J. (2011), "Rearch on design of aluminum truss bridge", *Adv. Mater. Res.*, **168-170**, 1776-1779.

https://doi.org/10.4028/www.scientific.net/AMR.168-170.1776.
Wen Q.J., Yue, Z., Zhou, M. and Liang, D. (2018), "Research on out-of-plane critical buckling load of upper chord in half-through truss bridge", *J. Huazhong Univ. Sci. Technol. (Natural Science Edition)*, **46**(1), 105-108. https://doi.org/10.13245/j.hust.180120.
Ye, J. and Lu, M. (2018), "Optimization of domes against instability", *Steel Compos. Struct.*, **28**(4), 427-438. https://doi.org/ 10.12989/scs.2018.28.4.427.
Zhang, F. and Huang, J. (1998), "Study of calculation method on lateral stability of top chord of half-through truss bridge", *J. Ningbo Univ. (Natural Science & Engineering Edition)*, **11**(2), 62-68.

BU